HEAVY IONS

W.J. Willis

CERN, PPE Division, 1211 Geneva 23

1. INTRODUCTION

We understand the title to be an abbreviation for the study of the condensed matter physics of hadrons, quarks and gluons at high density. The beams used so far are in fact not heavy ions but light ions or even protons.

Some of the recent results in this field were presented at the parallel session organized by Shoji Nagamiya, with a theoretical summary which was presented by Maurice Jacob. I have included a number of results presented two months before at the Quark Matter conference in Menton.

2. CONCEPTS

Fig. 1 shows an idealized version of the concept behind these studies. Two nuclei with large atomic number collide at a high energy and ideally deposit all of their energy into a Lorentz–flattened pancake of high density of energy and baryon number. This volume is promised by QCD to be a state where the quarks and gluons are deconfined, that is colour charge is allowed to move freely within the volume except for interactions between individual partons. Chiral symmetry will also be restored in these conditions. The high density state will then expand, particularly along the direction of incident beams where the pancake has its narrow dimension, and at some point a phase transition to a state of confined colour and broken chiral symmetry will occur. These particles will still interact among themselves until the density drops to a point, "freeze–out", where they are no longer interacting and depart to be recorded in our detectors. The energy density required to pass the transition is estimated to be one to two GeV/fm^3. Recall that the energy density inside a proton is about 0.5 GeV/fm^3. The deconfinement transition would also be passed by compressing nuclear matter at zero temperature, and in that case the baryon density required is expected to be five or six times the density of the nucleus (which corresponds to an energy density of about .14 GeV/fm^3).

3. BEFORE QCD

Before QCD and the theory of colour confinement were developed, the equation of state of hadronic matter at high densities was already required for calculations in cosmology and in fixing the properties of neutron stars. A theory was provided by Hagedorn, 30 years ago, in the context of mesons and nucleons, the statistical bootstrap model. In this theory the equation of state for high energy density is generated by an increasing level density of nucleon resonances. It was recognized that, at very high energy density, the principle would lead to the presence of hyperons and hyperon resonances as well. This theory gave a working model for the cosmologists, but is not very exciting from the point of view of experimental investigations. In the next step, T.D. Lee realized that chiral symmetry should be re–established at high densities and suggested the existence of a phase transition to "abnormal nuclear matter". Though much more interesting from the point of view of experiments, the theory was not well enough advanced to specify well where one should expect to find such a state or to determine its precise properties, and it did not lead to a determined experimental effort by high energy physicists to investigate heavy ion collisions. The well–determined Lagrangian in QCD, on the other hand, can in principle lead to precise confrontation with experiment, and the qualitative ideas are sufficiently clear to give us adequate notions of where to look and which signature of the phase transition to search for.

4. QUARK–GLUON PLASMA

Since we accept, provisionally, the Lagrangian of QCD, this field of investigation is not necessarily claimed to produce any new discoveries in fundamental interactions. A few words may be appropriate to justify our interest in this subject. First we note that the Universe has spent most of the size–doubling times of its existence in a deconfined state, passing into the hadron phase only at about 10^{-6} seconds. Furthermore, if the phase transition is of the first order with a considerable latent heat, as is likely, considerable spatial inhomogeneities will have been introduced in the mixed phase. It may be expected, for instance, that these inhomogeneities will have affected nuclear synthesis and thereby affected our estimate of the amount of baryonic matter in the universe. This effect might be sufficient to allow baryonic matter to explain the dark matter in the Universe.

Second, condensed matter physics, of which this is a novel sector, is widely considered to be one of the most beautiful parts of physics, and it is quite likely that effects will be seen in this variety of matter which will be novel and interesting in their own right. This is in harmony with the general programme of nuclear physics and offers better grounds for the continuation of the activities of traditional centres of nuclear physics than any other. Without such future directions, institutions and material and intellectual resources would in all probability be lost to science.

5. MILESTONES

When it was proposed to carry out a significant experimental programme aimed at these goals, well meaning critics pointed out a number of potentially severe impediments, to its success. I enumerate them below and when each difficulty has been overcome, I shall count a milestone passed, and organize this talk around the milestones.

(1) As the energy of the centre of mass is raised, hadronic matter becomes relatively transparent, even if the target is a heavy nucleus. In this case, the process of converting the kinetic energy of the projectiles into the disordered state of thermal energy density must grow increasingly inefficient. The first question is then whether a sufficiently high energy density can be achieved.

(2) The creation of a disordered state of very high energy density and the largest possible volume, necessarily implies that the final state of hadrons which we actually observe should consist of very many particles. This is a new experimental problem and it can be asked whether we can handle the difficulties of measuring the particles with sufficient precision, particle identification, and so on to extract the necessary information.

(3) Even though the gross indications of energy density may be present, it can be doubted whether the energy is really distributed over the degrees of freedom to a sufficient extent to allow a description in terms of bulk matter, much less thermodynamics and hydrodynamics. Tests must be devised to show whether this energy is indeed adequately distributed over the spatial degrees of freedom, and over other "chemical" degrees of freedom, such as the fraction of strange quarks compared to the equilibrium value.

(4) Given that energy is correctly distributed over all degrees of freedom, we still have to deal with very strong variations in time, and perhaps space. It can be asked whether for these transient states we can devise probes which are sensitive to the conditions at early times where the energy density was high, and the quarks and gluons deconfined.

(5) Last, can we use the observations made to establish some connection with the fundamental properties of QCD that inspired these investigations?

If we succeed in passing these milestones we will be able to speak legitimately of states passing along trajectories such as those shown in Fig. 2. We start with a cold nucleus and increase the energy and temperature along lines that are not dynamically defined, because of pre–equilibrium processes, arriving at a maximum which may or may not have passed the deconfinement boundary. The system then expands, dropping in density and temperature until confinement is re–established and the system eventually passes freeze–out. As shown in Fig. 2, at low energies the displacement is largely in the direction of a density increase with an accompanying increase in temperature. At very high energies, at least at the central region of the collision which is presumably not highly populated by the incident baryons, the displacement is mainly in the direction of increased energy density or temperature.

6. ENERGY DEPOSITION

The question of energy deposit was settled soon after the first SPS and AGS experiments four years ago. Fig. 3 shows the distribution of transverse energy over all rapidities created by sulphur projectiles at 200 GeV per nucleon on different targets. The curves derive from a simple model which evaluates the variation in the number of nucleon–nucleon collisions from the collision geometry, with a random distribution of impact parameters. It uses the known nuclear sizes and shapes. This model assumes a simple linear superposition of nucleon–nucleon collisions which is adequate to describe global quantities such as E_T, but fails when more detailed distributions are inspected. The numerical values of energy deposition depend on assumptions concerning the dynamics of the matter during or immediately after the collision. For example at the AGS energies, it is clear that all the kinetic energy is deposited in a slowly expanding reaction volume, but the shape of the volume at maximum compression still depends on dynamical assumptions. At one extreme is the Landau model, with a longitudinal expansion due to the high pressures generated. At very high energies where nuclear transparency is important an opposite limit is appropriate where there is no decelerating expansion but instead a flow of energy along the beam direction at the speed of light, as in a free expansion. The Landau model results in a Gaussian distribution of dE_T/dy while the high energy limit is characterized by a flat distribution in y. Formulas for the energy density in two cases have been given by Landau and by Bjorken.

A recent review by G. Stachel gives the values shown in Table 1. At 200 GeV, there is a wide uncertainty in the values of energy density, which may not be finally resolved until direct probes of initial energy density at short time are available, such as the thermal radiation of leptons pairs or real photons have been observed, though the strange quark fraction is also relevant. It is sufficient for our purpose to note that the values have entered the range where deconfinement can be expected. It is also noteworthy that energy density is definitely increasing still at 200 GeV per nucleon. M. Jacob at this conference also noted that the local energy density at the centre of the collisions region should increase by about a factor of two when one goes from a sulphur projectile to a lead projectile. The calculations of Kajantie for higher energy, which take into account the production of many jets show that as one goes from 200 GeV in fixed target, to the 200 GeV per nucleon in the centre–of–mass at RHIC, another factor of two in energy density should be obtained. The rapid increase in jet cross section should lead to still another factor of two or more in going to heavy ion beams in the LHC.

In summary, we have already entered the energy region where deconfinement can be expected, and during the next decade we should benefit from three additional powers of two as new facilities come into operation. Each of these factors in energy density is expected to increase, in some cases by up to an order of magnitude the size of the signal in the different probes considered below.

7. EXPERIMENTAL PROBLEMS

The problem of dealing with a large number of particles generated in these collisions has been met in a variety of ways. The measurement of E_T, for example, poses no particular problems since it can be done in a segmented calorimeter which naturally integrates over the large number of particles produced. The measurements of multiplicity do require increasing granularity as the number of particles goes up, but silicon pad technology and other tracking techniques have progressed so quickly that this does not present a major problem. Spectrometers of limited solid angle can always be designed so that the multiplicities to be dealt with are convenient. The ultimate challenge is to track all the particles created in the interaction. The reason for wishing to do this is primarily to observe short-lived strange particles and in particular the multiply strange hyperons such as Ξ^- and Ω^-. A new result presented at the conference shows complete tracking of the interaction of a silicon beam on a gold target, seen in a time projection chamber in the BNL MPS, as shown in Fig. 4. The hit display looks quite dense, but since in a TPC space points are created, the tracking routines are very powerful. A demonstration that satisfactory results were achieved is shown in Fig. 5 which shows the mass distribution for the V^0's in these events. The width of the mass distribution, and the acceptance corrected lifetime distributions are satisfactory, illustrating that even this problem can be solved.

8. EQUILIBRATION

In order to utilise the energy density in our investigations, it is essential that the energy be adequately distributed over the degrees of freedom of the system. A first necessary condition is that the distributions at the transverse mass should be approximately consistent with the exponential behaviour characteristic of the Boltzmann distribution and that the slopes agree for the different particle species. Recent results from the NA35 streamer chamber experiment for 200 GeV S+S collisions are shown in Fig. 6 and results from the WA85 Omega spectrometer for S–W collisions in Fig. 7. The various slopes are nearly equal.

An interesting result is obtained in the NA34 external spectrometer where it is shown, Fig. 8, that the slope is very nearly the same for negative particles, presumably pions, produced in p–W and S–W collisions. This was not the result expected. It had been supposed that the distributions generated in hadron collisions, while of the exponential form, did not represent a true thermal distribution and therefore when they underwent further secondary collisions in the larger collision volume created by a heavy projectile, that they would relax toward the equilibrium form by the Boltzmann mechanism, since only a few collisions are sufficient to achieve this thermalization. The moderate size projectiles currently used should already be sufficient to accomplish this. The fact that there is very little change has been pointed out by Shuryak as a paradox: either there is some precocious approach to thermal equilibrium in proton–proton collisions or a different universal mechanism which creates the same slope or a fortuitous coincidence of some precision.

9. STRANGENESS

We may ask whether the fraction of strange quarks is that calculated for an equilibrium distribution at the temperature determined from the slopes of the energy spectra, taking into account the higher mass of the strange quark, so–called chemical equilibrium. This is a stringent test of the distribution of energy over degrees of freedom, since kinetic calculations indicate that it takes many more collisions to establish chemical equilibrium than thermal equilibrium. This is because every collision randomizes the momentum components of a proton to some extent, but only a fraction creates new strange–quark pairs. New evidence on this matter has been presented to this conference by the NA35 experiment on neutral strange particles, as shown in Figs. 9 and 10. It is seen that the ratio of strange particles to negative particles, which are mostly pions, rises as the number of particles in the event increases. For peripheral events with a small number of created particles, the ratio is similar to that for a proton collision with the same target nucleus. This is itself similar to the value seen in nucleon–nucleon collisions, or to the models based on superposition of nucleon–nucleon collisions. For events with large numbers of produced particles corresponding to central collisions, the enhancement of strange particles is of the order of a factor of two. Fig. 11 shows the fraction of strange quarks λ, a parameter which has long been used in hadron collisions, showing the same enhancement. This value of λ is close to that obtained from a calculation for the chemical equilibrium of strange quarks, at a temperature corresponding to the observed slopes of the energy spectrum.

An extensive set of data has been obtained by the E802 experiment at the AGS, and presented at this conference, Fig. 12. It again shows an enhancement of about a factor of two comparing proton gold and silicon gold central collisions. Also shown is the enhancement going from proton–berylium to proton–gold, for an overall increase of about a factor of four. Note that the rapidity peak for K^+ in silicon–gold collisions is shifted in the direction of the target frame, as is the distribution of protons. This indicates the tendency of high baryon density to influence the enhancement in strangeness, a quark–gluon plasma probe to be mentioned in the next section.

It has also been stated by Rafelski and others that it is relatively difficult to obtain chemical equilibrium in a hadron gas, because of the small cross section for pion collisions to produce kaon–

pairs. It is fair to say that there was a genuine prediction of the attainment of chemical equilibrium, due to the presence of quark–gluon plasma, where the cross section for two free gluons to produce a q–$\bar{q}$ pair is quite large. Of course, we do not really know the physics of a hypothetical hadron gas of very high density: perhaps there the strangeness production would be much larger than anticipated. The result does seem to indicate some new physics at work.

10. PRODUCTION OF MULTIPLE STRANGENESS

Given that it has been established that we are dealing with high energy density states with the energy–distributed over all degrees of freedom, we may legitimately test the specific predictions associated with the quark–gluon plasma state. The oldest of these predictions (Rafelski) is based on the assumption, valid for the present experiments at the SPS and especially the AGS, that we are dealing with a system with large net baryon number. In that case, a system of quark gluon plasma, the free u and d quarks fill up the states available in phase–space and the production of antiquarks is enhanced, particularly the strange antiquarks. The formation of anti–hyperons is thus enhanced, and the production of multiply strange anti–hyperons (relatively rare in ordinary collisions) should be a particularly striking signal of this state. Rafelski argues that the annihilation of the anti–hyperons in a final hadronic phase will not much dilute the signal. Accordingly he recommends measurement at the ratio of $\bar{\Xi}^-/\Xi^-$, comparing for example S–W collisions and p–W collisions, as well as the corresponding ratio for the singly–strange hyperons such as $\bar{\Lambda}$.

These are difficult experiments, requiring reconstruction of essentially all the tracks in the event in order to obtain the V–particles and the associated π^- decay tracks in the case of the Ξ^-. A visual or quasi visual method, like the TPC, is required. The NA35 streamer chamber experiment has reported on the $\bar{\Lambda}$ experiment at this Conference, Fig. 13.

11. ANTIBARYONS

More recently John Ellis has noted that the high temperature chiral state as it lowers its temperature has a tendency to form baryon–antibaryon pairs. These ideas have been extended by A. Mueller who finds that baryon–antibaryon pairs can be enhanced over the ordinary value by an order of magnitude. Of course, in the hadronic phase there will be some annihilation, which has been estimated in a recent calculation from the Helsinki group, who obtain the following formula

$$R_{\text{Annihil.}} = \left(\frac{\tau_o}{\tau_f}\right) \frac{\langle \sigma_a v \rangle}{\pi RL} \left[\frac{dN_B}{d_y} - \frac{dN_{\bar{B}}}{dy}\right]$$

where τ_0 is the hadronization time,

τ_f is the freeze out time

and σ_a is the average annihilation cross section.

Using a baryon density from the Attila event generator, they obtain the annihilation factor shown in Fig. 14. This shows that the observed antibaryons should be corrected upward by a significant factor and that the residual fraction observed should be strongly peaked in the central rapidities, where the baryon number is relatively low.

The strangeness and chiral enhancements may combine, since we expect the chiral based transition–boundary and the deconfinement phase–transition boundary to be rather close, so that the trajectory of our experimental state will cross both of them. Thus we see that there are two reasons why anti–hyperons should be enhanced, the chiral enhancement applying to all antibaryons, the strangeness argument enhancing the anti–hyperons and particularly the multiply–strange anti–hyperons.

The NA35 result, with limited statistics, seems to show that the $\bar{\Lambda}$ is enhanced over the value obtained with proton beams, even more than the Λ, and even without a correction for final state annihilation.

The WA85 experiment is an adaptation of the Omega Spectrometer set to observe hyperons at substantial angles to the beam, where the particle density is reduced. The hyperons have $p_T \geq 1$ GeV. It has succeeded in the difficult task of measuring Ξ's and $\bar{\Xi}$'s. The result is given below.

$$\bar{\Xi}/\Xi = \begin{cases} \text{S–Pb } 53/123 = 0.43 \pm 0.07 \\ \text{p–W } 22/82 = 0.27 \pm 0.06 \end{cases}$$

This shows an effect in the predicted sense. It is still limited by a statistics but a factor of five in statistics is on the way. We conclude that these predictions are supported by the present data.

12. RADIAL EXPANSION

As far as the general level of antibaryons, we have available the rather complete set of particle spectra obtained at the AGS by the E802 experiment (Fig. 15). This shows substantial fluxes of antiprotons, reduced by a factor of about three from the values obtained with proton beams, but in the environment of high baryon density of these experiments one might have expected large annihilation corrections. In further inspecting this figure we note that at this energy there are large differences in the slopes of the energy spectra for different particles. This is suggestive of coherent radial motion. We recall that some time ago, in the collisions observed at the Bevalac at 1 to 2 GeV per nucleon, a coherent radial motion, or "blast wave", was observed. This is easily understood at that energy, where the nucleons scattering manifest a hard core. The two projectiles deliver energy into a gas of nucleons which is transformed by random scatters into an outward gradial motion. For a nearly massless particle such as a pion, this produces a change of the spectral slope, producing a false measurement of the temperature due to the combined effect of thermal motion and radial motion. In the case of a massive particle such as the proton the radial velocity produces a distortion of the energy spectrum and the change in slope is much greater.

It would seem that some element of this effect persists at AGS energies, but largely disappears as the energy is raised to 200 GeV. If the disappearance of this effect is abrupt as the beam energy is increased, it might be related to the crossing phase boundary of the deconfinement transition.

13. THE MELTING OF THE J/ψ

The disappearance of the J/ψ is a well known consequence of the quark gluon plasma predicted by Matsui and Satz. It was previously noted by Pisarski that Debye shielding keeps vector mesons from being bound in QGP. The application of this idea to particles like the ρ is frustrated by the fact that they will be reformed in the later, hadronic phase. The above authors noted that in the case of the J/ψ it is unlikely that the relatively rare $c\bar{c}$ quark pair will find partners in the hadronic phase. They noted that this will lead to a J/ψ suppression in collisions with high E_T and in particular for J/ψ with low p_T. This prediction was beautifully confirmed by the NA38 experiment at the CERN SPS. Fig. 16 shows how the number of J/ψ (compared to the continuum) decreases as E_T is increased and Fig. 17 shows that the effect occurs at small p_T. A new observation shows (Fig. 18) that the form of the continuum does not change with E_T, so that the effects are peculiar to the J/ψ.

Subsequently, many authors have been able to construct models using combinations of initial state and final state interactions which do the same job. At this Conference a paper of Capella et al. shows a fit simultaneously to the pA J/ψ data and to the ^{16}O J/ψ data with a J/ψ–proton cross-section of about 6 mb. This large J/ψ cross section, which is the key to the effect, they explain as a kind of string–string interaction, schematically illustrated in Fig. 19. In this case, as in many of these models, there is some interesting new physics invoked to produce the effect.

Even though there are many models which can very plausibly explain the effect, the confirmation of the prediction of Matsui and Satz has had a substantial impact. This is perhaps due to what we might call the predictive paradigm, whereby we tend to accord an increased significance to results which follow a prediction. It is clear that a single prediction of this type cannot lead to a decisive demonstration of the existence of the QGP. Better data on these reactions will still be very helpful to see whether, for example, the production of J/ψ levels off as p_T is increased further, or continues to rise, contrary to the prediction. It would also be valuable to see whether the effect has an energy threshold, and how it behaves with larger projectiles.

14. FUTURE DIRECTIONS

A number of the most promising distributions for making direct contact with QCD have not yet been brought to the stage of experimental test. Since they are quite important for the development of the field in the next few years, I list them here with brief comments:

(1) Single particle distributions need to be measured over the whole volume of experimental parameters in order that the pattern due to QGP effects may become evident. These include the fraction of anti–baryons, the relative fraction of anti–hyperons and anti–cascade hyperons and the strength of the blast–wave, the signature of coherent radial expansion. While it should be possible to turn the effects on and off by varying the transverse energy for a given projectile and beam energy, in so doing we vary the event geometry as well as energy density, which may blur any sharp thresholds. It will be a valuable complementary method to vary the centre–of–mass energy for fixed impact parameter. It is often rather inconvenient to do that in fixed target experiments, but when in collider experiments energy scans become available, thresholds in energy due to the onset of QGP may become much more evident.

(2) If the QGP phase transition is of first order with a large latent heat, (or with a large change in the free energy over a small range of temperatures even if *not* first order) we may expect a clear experimental signal in the measured value of the lifetime of the hadronic state by means of meson intensity interferometry, the Hanbury–Brown and Twiss effect. This effect has been predicted by Sinyukov, Pratt and Bertsch. In essence, hydrodynamic calculations show that it takes a relatively long time to dissipate the energy of a phase transition, and this can be detected in the correlation function of identical mesons, specifically in the component related to the energy difference of two pions emitted at nearly the same direction. This correlation function is expected for the dissolution of a hadron gas to be of the same width as that corresponding to the spatial extent, described by the correlation of two pions with similar momenta and different angles. For the long lifetime phase, on the other hand, the correlation function can the narrower, corresponding to a longer lifetime, by a factor of two to five. Such a measurement requires very good statistics and extremely good momentum resolution.

15. THERMAL ELECTROMAGNETIC RADIATION

An experiment which has been much discussed but for which we have few results, is the emission of thermal lepton pairs, or the corresponding real photons. To see the emission of thermal radiation above the background due to single quark processes, a very large energy density is expected to be required. Calculations with a moderate degree of optimism show that it is not an easy signal at SPS energy, but may become substantial at collider energies, especially for collisions of heavy ions in the LHC, Fig. 20.

The information carried by lepton pairs or photons is particularly valuable in that it gives a possibility of a clear characterisation of the collision at very early times, when the energy density is at its maximum, and the blurring effect of hadronisation has not yet set in.

Leptons pairs are also a tool useful in searching for quasi particle effects. In the recent Quark Matter conference, a paper by Weldon shows that in certain models a plasmino state can give rise to a sharp peak in the two lepton spectrum at low mass values, for masses less than the transition temperature, shown in Fig. 21. Such effects would be very striking indeed. Other authors have discussed signals in a similar energy range due the dispersion relation of pions in nuclear matter. It is interesting, in this connection, to see the first results of an experiment at the BEVALAC, in a regime of relatively low pion mode multiplicity and high baryon density, which shows possible signs of structure (Fig. 22). The same group has pointed out evidence of structure already in proton–berylium data.

16. CONCLUSION

Having just mentioned that many studies are expected to be more rewarding at higher energies, it is useful to review the remarkable circumstance that in short space of time in the near future the available energy is slated to increase by a factor which is unprecedented in hadron accelerator facilities. Fig. 23 shows the energy in the centre of mass versus time for facilities in the past and predicted to come on line in the remainder of this decade. This plot is similar to the well known Livington plot for photon collisions, but we find that in order to obtain a straight line we must plot not the logarithm of the energy, as in the former case, but the logarithm of the logarithm of the energy. We should probably not count on extrapolating the curve very far.

In conclusion we may say that given the plethora of results from a rather small experimental programme, and that we have passed three or four of the hardest milestones, and noting the extraordinary new facilities coming on line in the next few years, we may safely say that the 1990's offer a fabulous richness of experimental opportunities in this field.

Table 1: Stachel Review, QM 90

E_{LAB}.A GeV	SYSTEM	ε_{BJ} GeV/Fm^3	ε_{Landau} GeV/Fm^3
14.6	Si + PB	1.	1.1
200	S + W	2.7	8.3

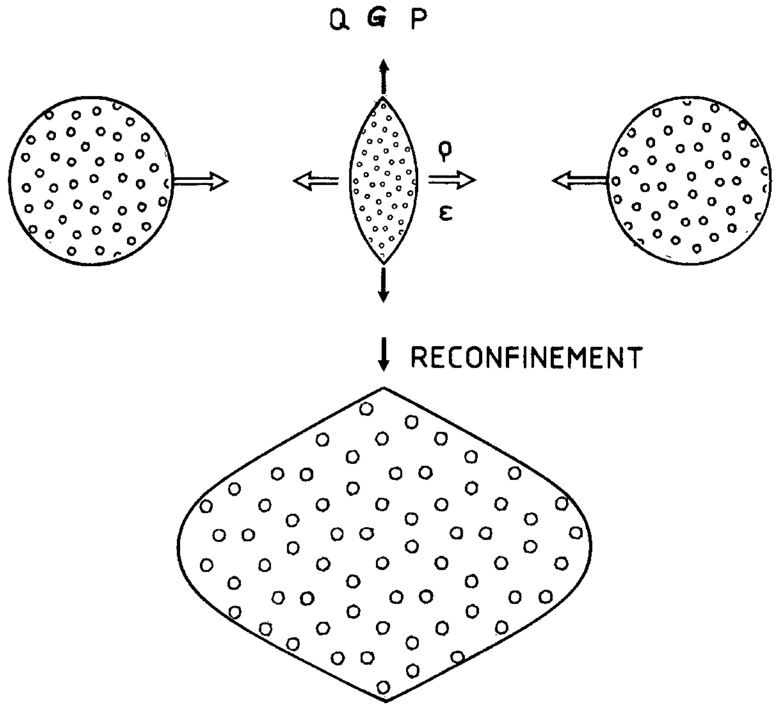

Fig. 1 Schematic view of the collision of two nuclei producing a region of high energy density which then expands longitudinally.

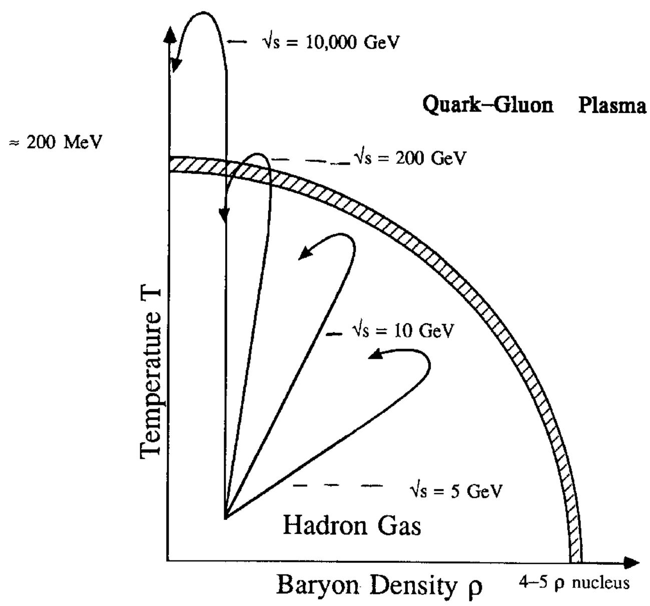

Fig. 2 Thermodynamic trajectories estimated for collisions at different centre–of–mass energies showing the creation of quark gluon plasma for the higher energy collisions. Maximum baryon density occurs for the lower energy collisions.

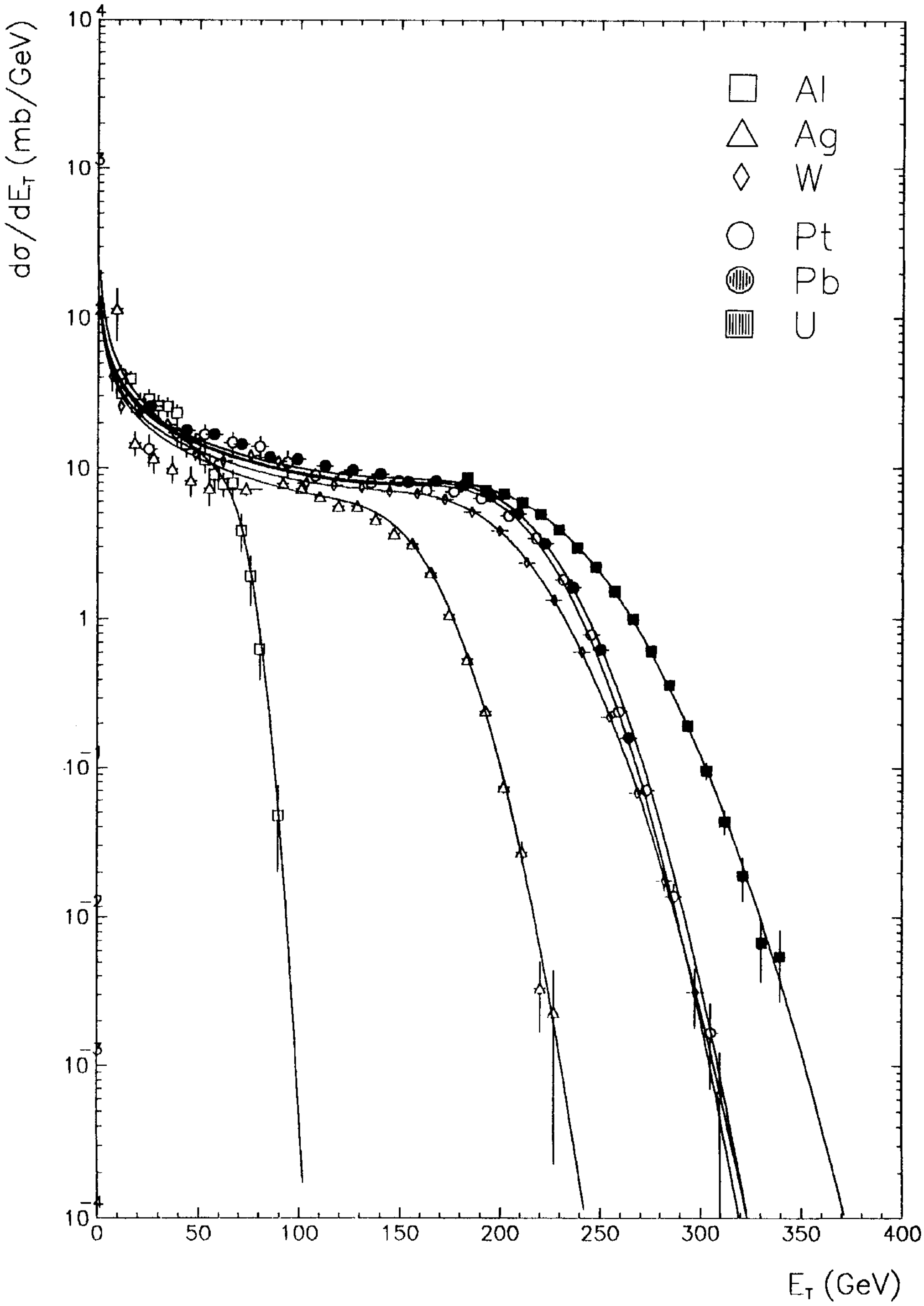

Fig. 3 Transverse–energy differential cross–section $d\sigma/dE_T$ in the rapidity range $-0.1 < \eta < 5.5$ for a 200 GeV/n ^{32}S beam on various targets (NA34). The full lines correspond to a parametrization with a geometrical model (see text).

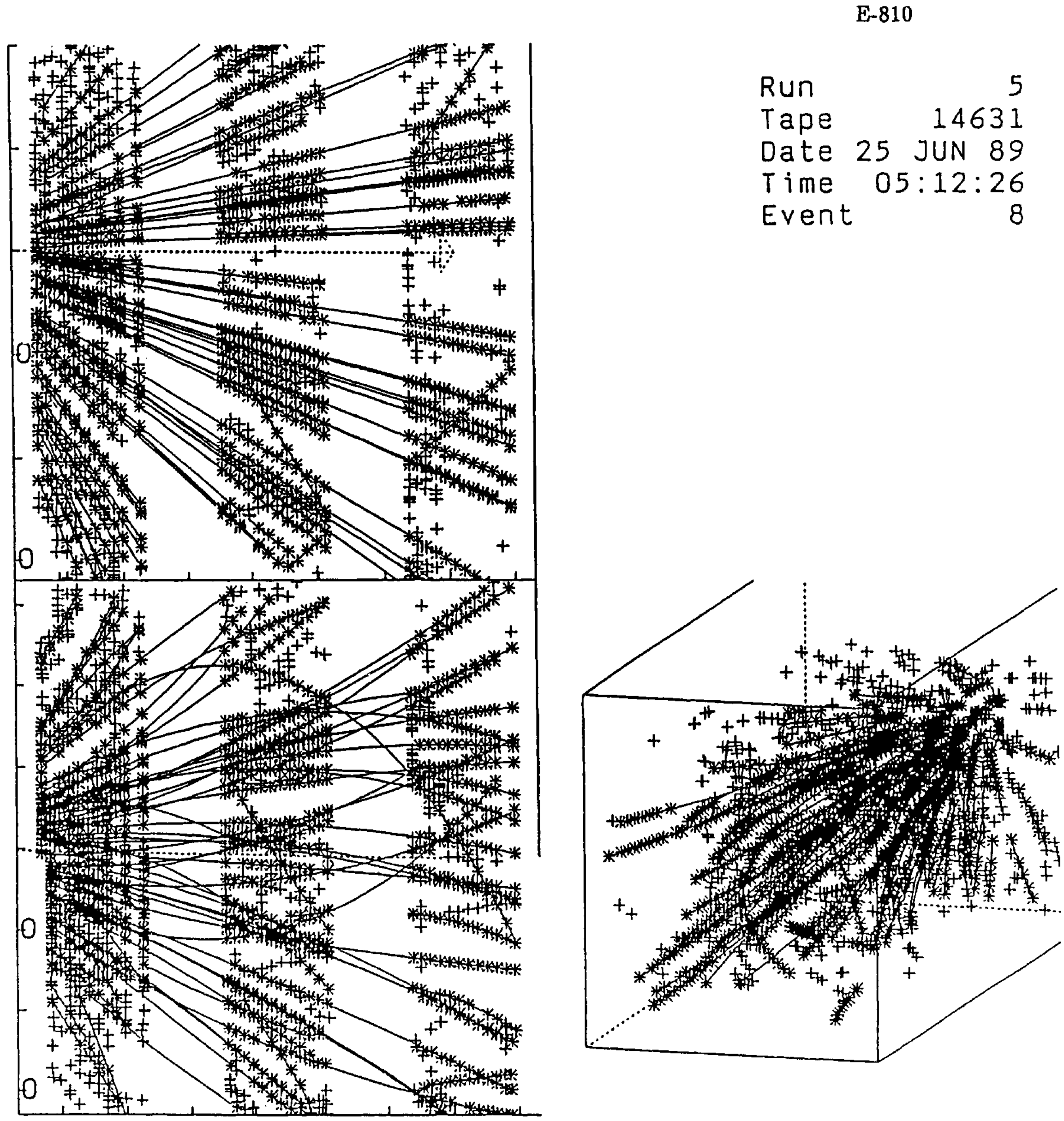

Fig. 4 Reconstructed tracks from a silicon–gold collision detected in the E810 TPC.

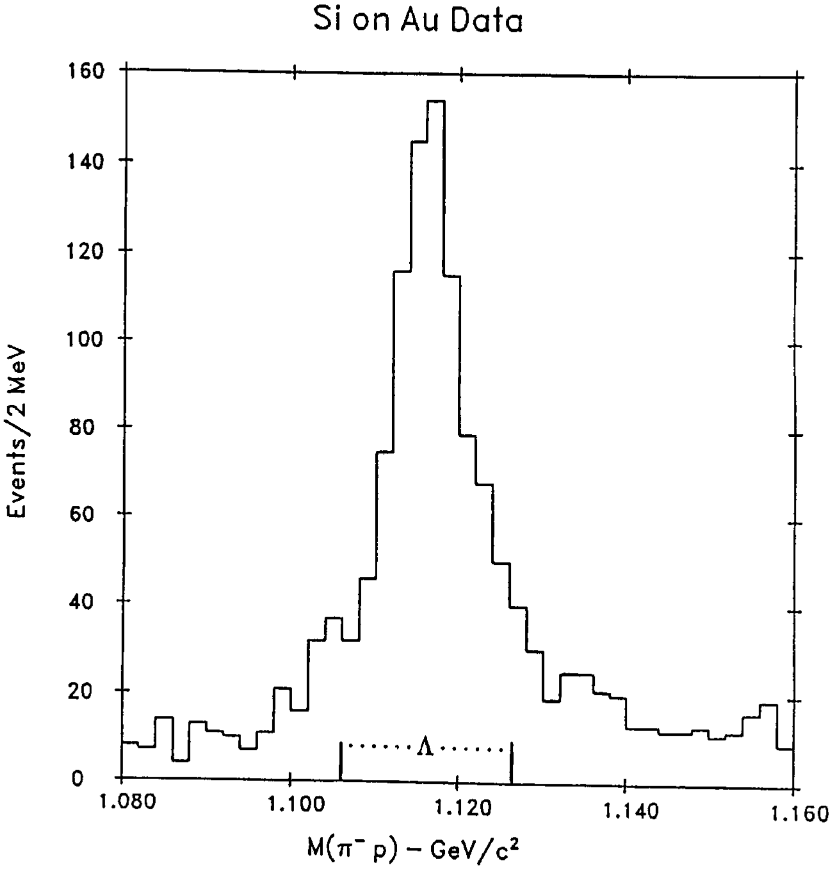

Fig. 5 Invariant mass spectrum of π–p for V° decays in 14.5 GeV/n Si + Au reactions (E810).

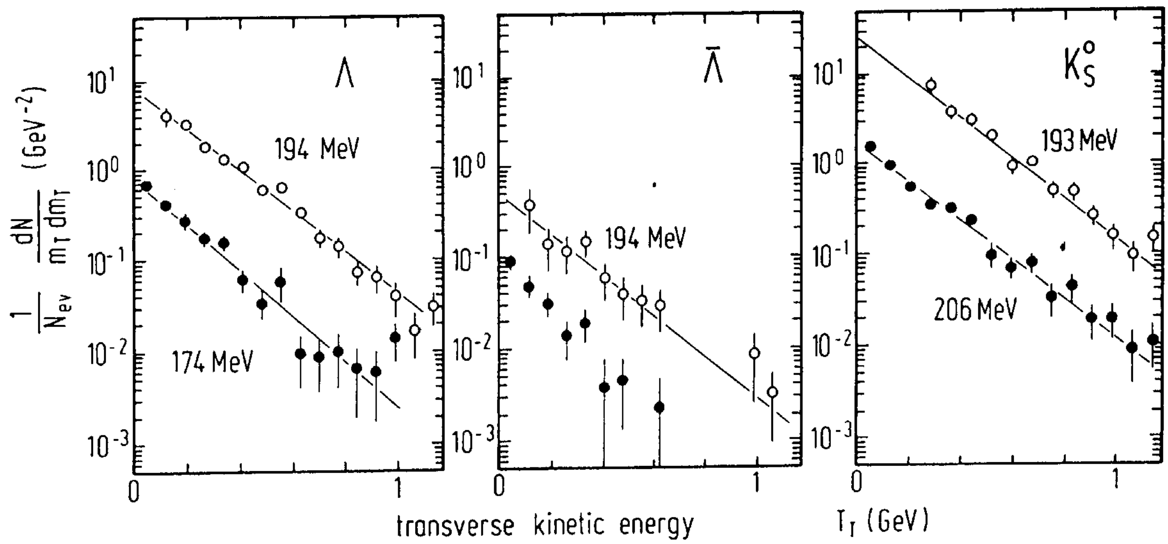

Fig. 6 Transverse kinetic energy spectra for neutral strange particles in central S+S (open circles) and p+S (full circles) collisions. The inverse slopes of exponential fits to the data (full lines) are indicated in the figure (NA35).

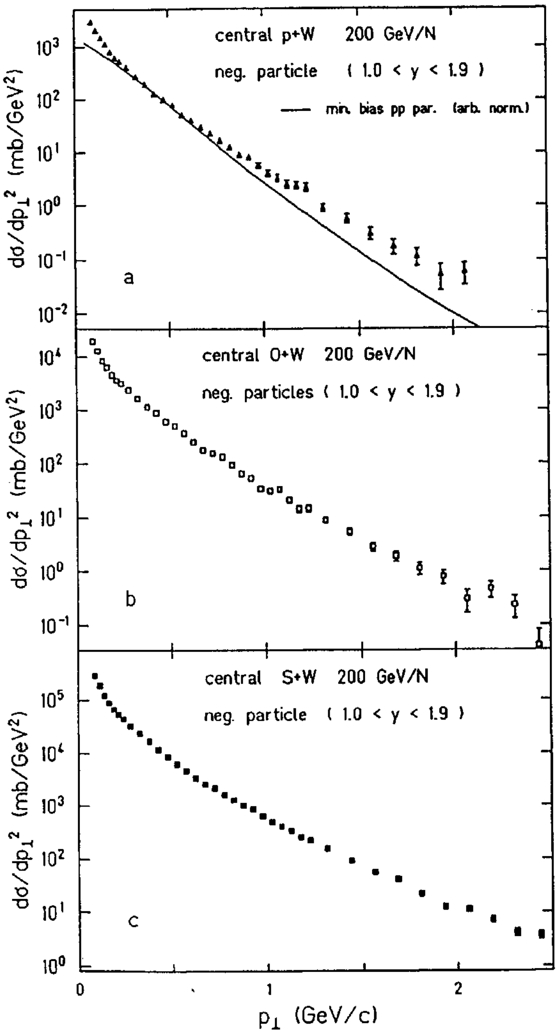

Fig. 8 Transverse momentum spectra of negative particles in central p+W, O+W and S+W collisions (NA34). For comparison, a parametrization of pp data is shown as a full line.

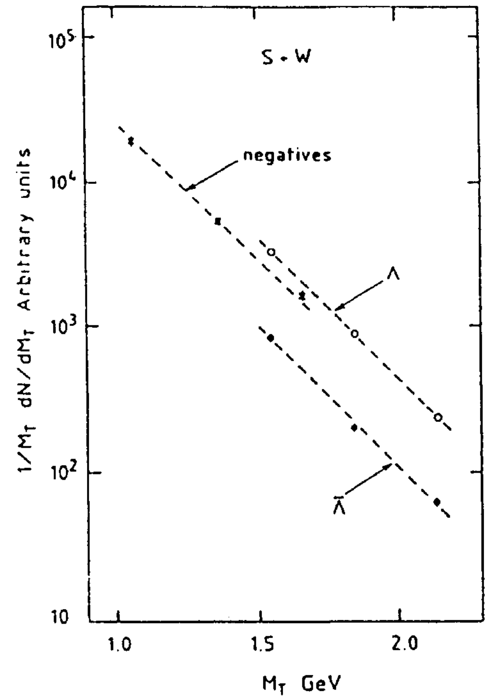

Fig. 7 Transverse mass spectra of negative particles, Λ and $\overline{\Lambda}$ in central S+W reactions at 200 GeV/n (WA85). The full lines, corresponding to an inverse slope of 230 MeV, are to guide the eye.

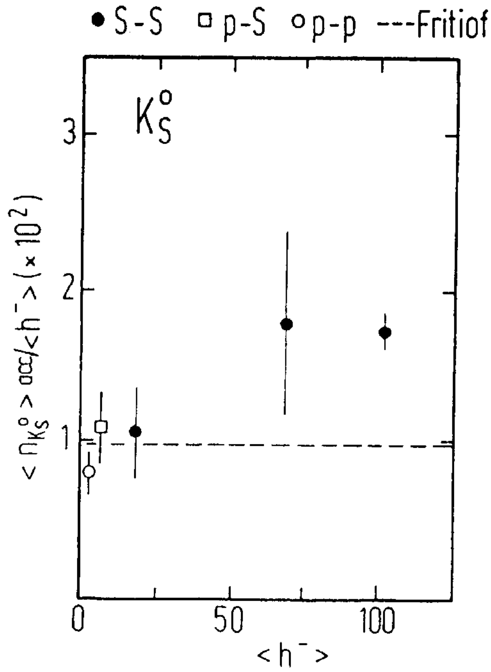

Fig. 9 Ratio of the mean multiplicity of K^o_{short} to the total negative hadron multiplicity h^- in peri–pheral, intermediate and central S+S reactions (full circles). Open circles are for pp and open squares for min. bias p+S collisions, the full line represents the Fritiof prediction (NA35).

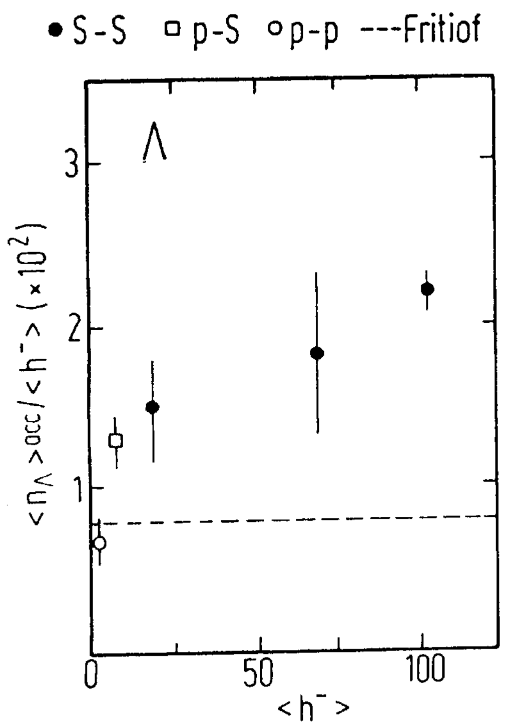

Fig.10 Same as Fig. 9 for Λ.

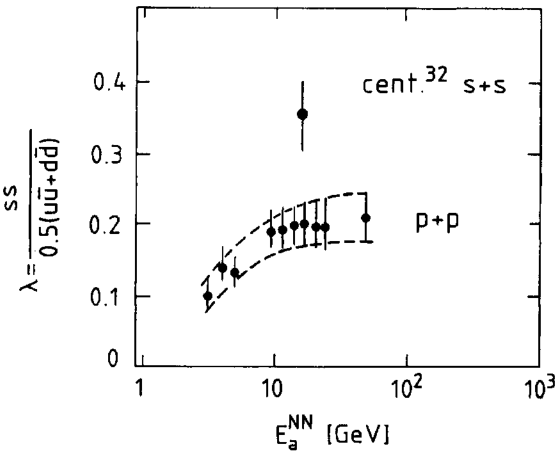

Fig.11 Strangeness suppression parameter λ as a function of the centre–of–mass energy in the nucleon–nucleon system for pp and central S+S collisions (NA35).

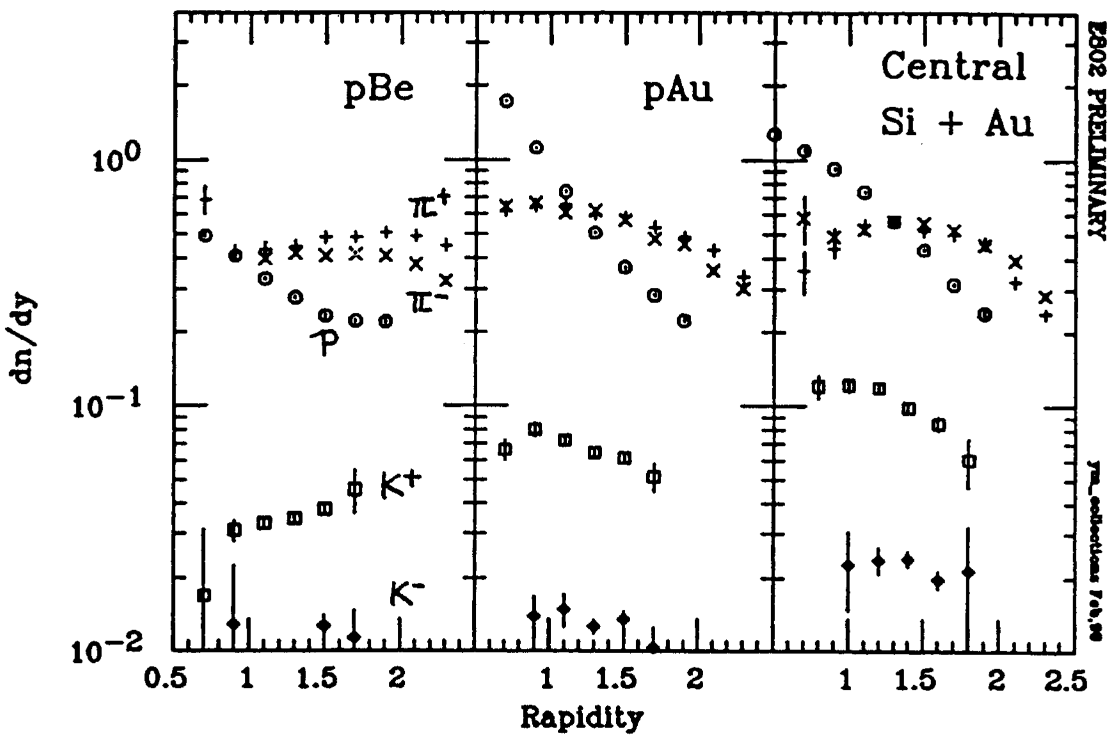

Fig.12 Rapidity distribution for $\pi^\pm$, $K^\pm$ and protons in p+Be, p+Au and central Si+Au collisions. The Si+Au data are divided by 28 (E802).

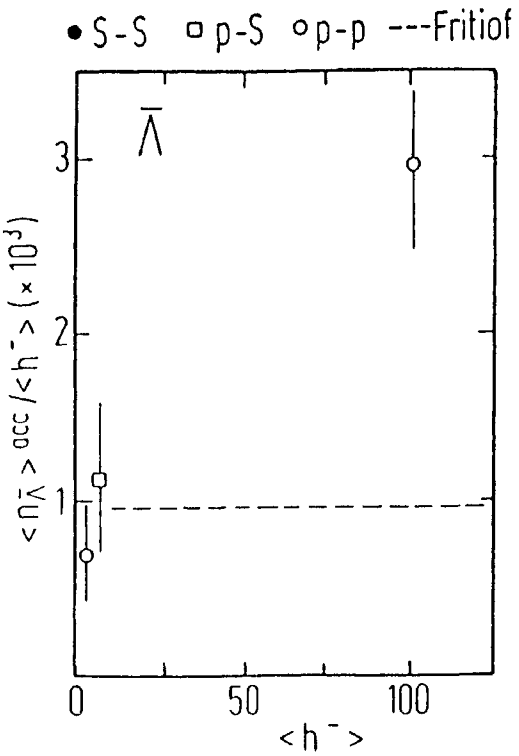

Fig.13 Same as Fig. 9 for $\bar{\Lambda}$.

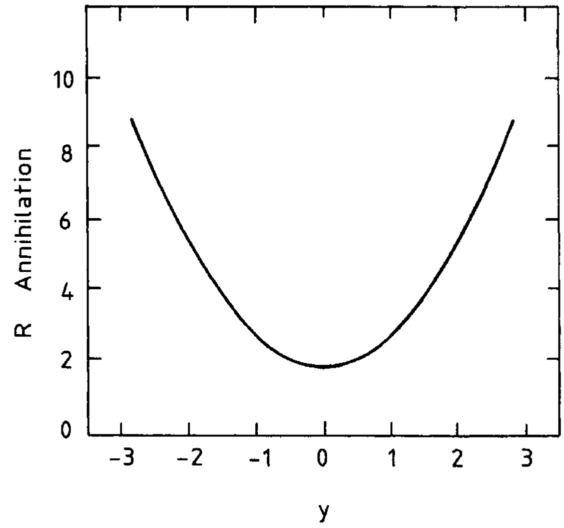

Fig.14 The factor by which antibaryons are reduced by final state annihilation as a function of rapidity.

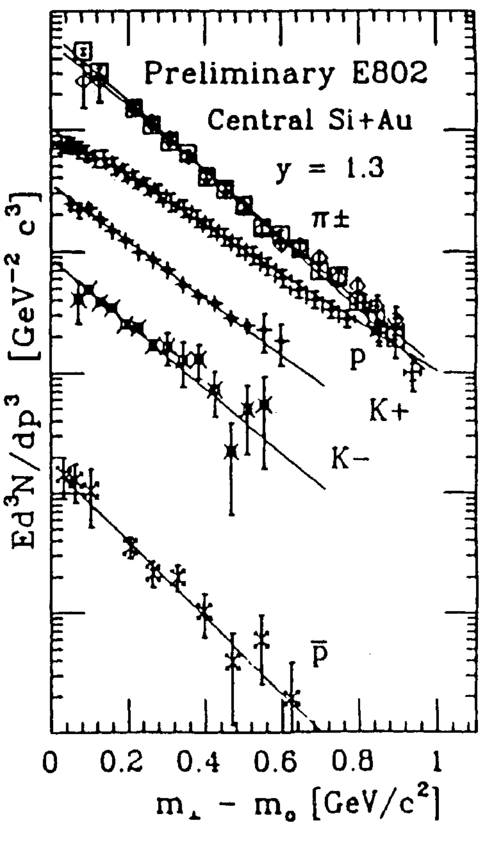

Fig.15 Transverse kinetic energy spectra for produced particles at y = 1.3 in central Si+Au reactions (E802).

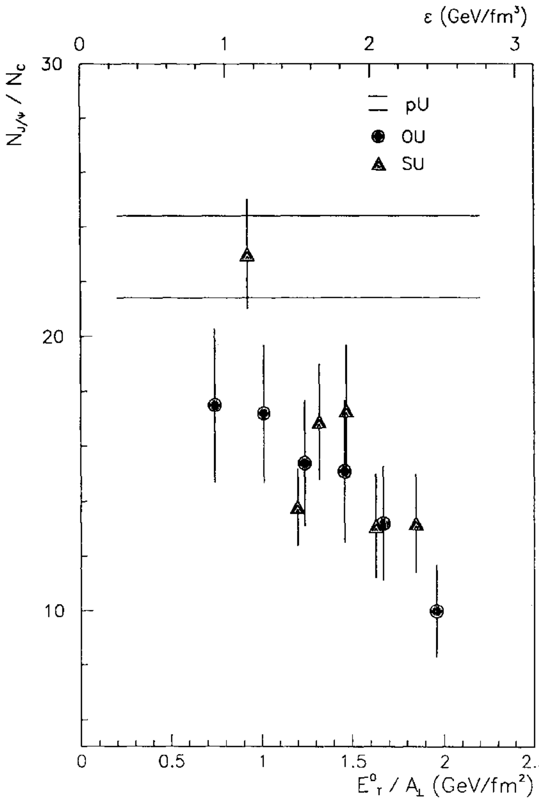

Fig.16 J/ψ to continuum ratio as a function of neutral transverse energy divided by the area of overlap between the nuclei. This quantity is proportional to the Bjorken energy density ε (upper abscissa) (NA38).

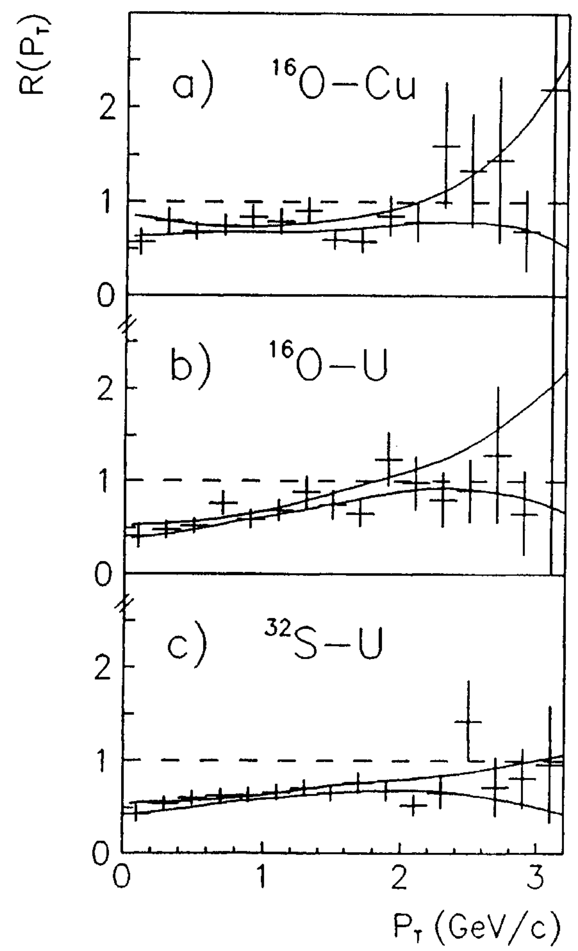

Fig.17 J/ψ suppression as a function of p_T (NA38).

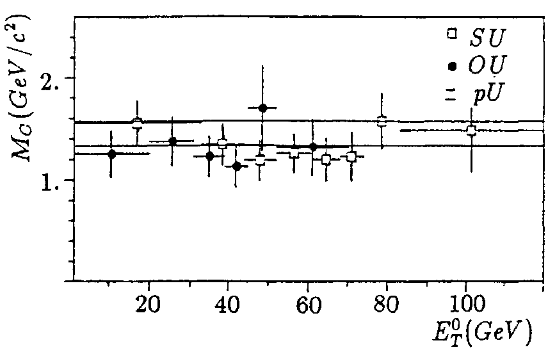

Fig. 18 Mass slope parameter of the continuum around the J/ψ as a function of transverse energy (NA38).

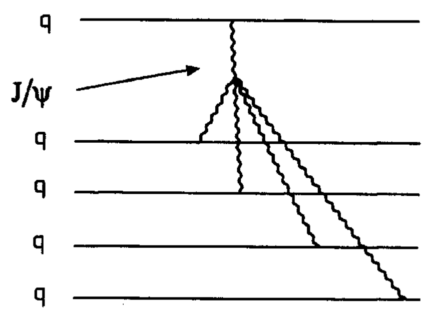

Fig. 19 The diagram showing the origin of the enhanced initial/final state interaction in the calculation of J/ψ suppression of Capella et al.

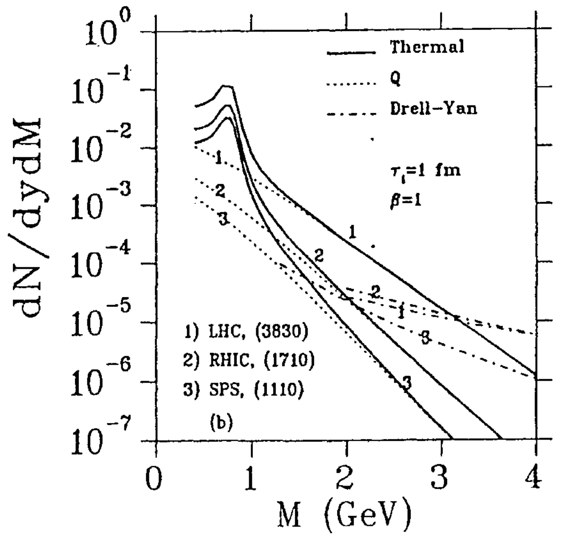

Fig. 20 Dilepton spectra for central Pb+Pb collisions at SPS, RHIC and LHC energies (pion multiplicities per unit of rapidity are given in brackets). Q indicates the contribution from the plasma above the critical temperature T_c = 160 MeV.

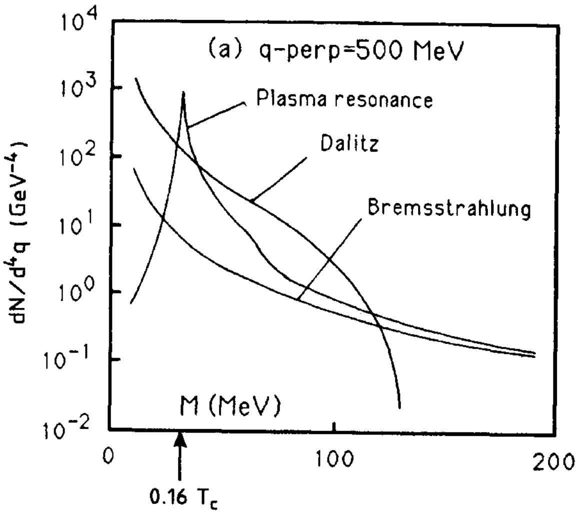

Fig. 21 Mass spectrum dN/d^4q (GeV^{-4}) of e^+e^- pairs. For q_T = 500 MeV the plasmon resonance at M = 0.2 · T_c = 40 MeV is slightly above the Dalitz and bremsstrahlung backgrounds.

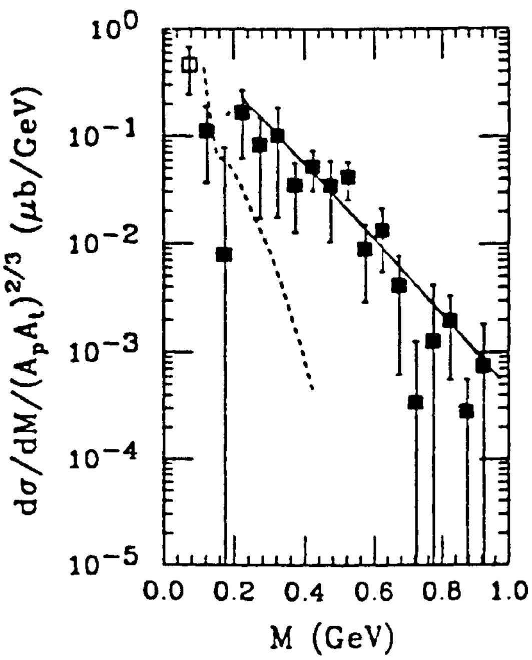

Fig. 22 Dilepton spectrum for Ca+Ca collisions at 1 GeV/n (DLS). The dashed curve represents the contribution from Dalitz decays, the solid line is an exponential fit for M > .2 GeV.

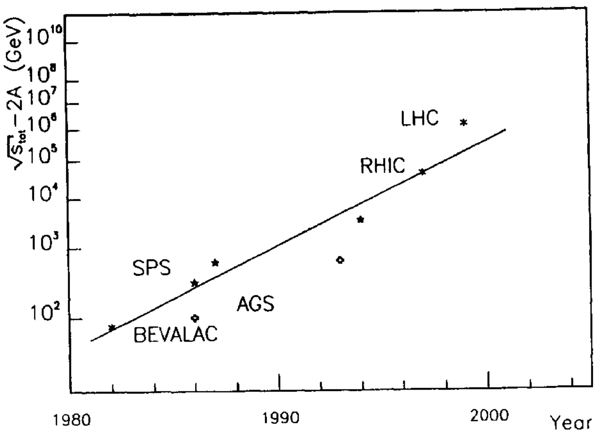

Fig. 23 Total laboratory equipvalent energy of various heavy ion accelerators as a function of year of turnon.